

Cite this: *Dalton Trans.*, 2024, **53**, 33

Josef T. Boronski

Received 24th October 2023,  
Accepted 27th November 2023

DOI: 10.1039/d3dt03550f

rsc.li/dalton

## Alkaline earth metals: homometallic bonding

## Introduction

Group 2 of the periodic table – the alkaline earth (Ae) elements – comprises a unique cast of characters. The lightest group member, beryllium, is one of the rarest elements in the universe as it is consumed by fusion reactions in stellar interiors.<sup>1</sup> Given their remarkably low density and high stiffness, beryllium alloys (and the metal itself) find applications in aerospace engineering.<sup>2</sup> Radium, the heaviest (reported) Ae element, is radioactive and has no stable isotopes.<sup>3</sup> As a result, <sup>223</sup>Ra ( $t_{1/2}$  = 11.43 days), which is a potent  $\alpha$ -particle emitter, has found use in radiopharmaceuticals.<sup>4</sup> In contrast to these two exotic metals, the other alkaline earth elements – mag-

nesium, calcium, strontium, and barium – are all rather abundant and cheap.<sup>5</sup> Hence, from the perspective of sustainability, the use of Ae elements to facilitate industrially relevant chemical transformations is attractive, and has received considerable attention in recent years.<sup>5,6</sup>

Decamethylzincocene – the first stable complex of zinc(i) with a Zn–Zn bond – was reported in 2004.<sup>7</sup> Due to the diagonal relationship between zinc and magnesium, this discovery inspired both synthetic and theoretical chemists to investigate whether the isolation of complexes with homometallic alkaline earth metal–metal (Ae–Ae) bonds might be possible.<sup>8</sup> Consequently, in 2007, the frontiers of molecular Ae chemistry were redefined by the report of  $[(^{\text{Dipp}}\text{Nacnac})\text{Mg}]_2$  (**1**;  $^{\text{Dipp}}\text{Nacnac} = \{[(\text{Dipp})\text{NC}(\text{Me})_2\text{CH}]^-\}$ , Dipp = 2,6-diisopropylphenyl) and  $[(^{\text{Dipp}}\text{Priso})\text{Mg}]_2$  (**2**;  $^{\text{Dipp}}\text{Priso} = \{[(\text{Dipp})\text{N}]_2\text{C}[\text{N}^{\text{i}}\text{Pr}_2]\}^-$ ) – stable complexes of magnesium(i) which feature Mg–Mg bonds (Fig. 1).<sup>9</sup> In subsequent years, numerous complexes with Mg–Mg bonds have been prepared, their reactivity has been intensively investigated, and the nature of the Mg–Mg linkage has been probed by a range of computational and analytical methods.<sup>10–12</sup> Indeed, magnesium(i) dimers have been described as “quasi-universal” reductants for chemical synthesis.<sup>13</sup> However, despite the increasing ubiquity of complexes with Mg–Mg bonds, efforts to prepare homometallic

Chemistry Research Laboratory, Department of Chemistry, Oxford, OX1 3TA, UK.  
josef.boronski@sjc.ox.ac.uk



Josef T. Boronski

Josef completed his undergraduate degree at the University of York in 2017 and subsequently undertook a PhD with Prof. S. T. Liddle at the University of Manchester. In 2021, Josef began a Junior Research Fellowship at St John's College, University of Oxford, hosted in the laboratories of Prof. S. Aldridge. Josef's research interests include the synthesis and reactivity of main group and actinide complexes, which feature low-valent element

centres or unusual bonding linkages. In 2023, he received the Dalton Emerging Researcher Award by the Royal Society of Chemistry.

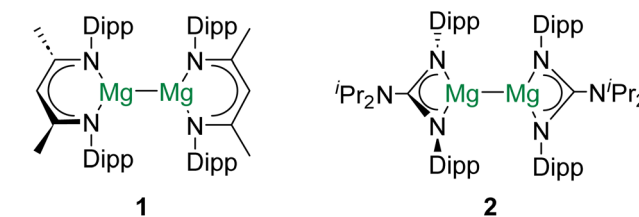


Fig. 1 Magnesium(i) dimers **1** and **2**. The first isolated complexes that feature Ae–Ae bonds.



bonds involving other Ae elements have been, until very recently, unsuccessful.<sup>14–16</sup>

This article will review recent advances in the field of alkaline earth homometallic bonding. It also seeks to highlight lessons from theoretical investigations into Ae–Ae bonding, as well as those from other blocks of the Periodic Table. Thus, it is hoped it will inspire new approaches to the synthesis of complexes with Ae–Ae bonds.

## Bonding considerations

Numerous theoretical investigations into the stability of complexes of the type XAeAeX, with two alkaline earth metals in the +1-oxidation state and an Ae–Ae bond, have been published.<sup>8,17–21</sup> Many highlight the need for bulky X-groups, which kinetically stabilize the Ae–Ae bond and inhibit disproportionation to AeX<sub>2</sub> and Ae. Data for the dimetalloenes, CpAeAeCp (**3Ae**; Ae = Be, Mg, Ca, Sr, Ba), are presented in Table 1.<sup>19</sup> In all cases, in the gas phase, the disproportionation of **3Ae** into divalent MCP<sub>2</sub> and atomic M ( $\Delta E_{\text{DP}}$ ) is endothermic. However,  $\Delta E_{\text{DP}}$  for **3Mg** (58.2 kJ mol<sup>-1</sup>) is around 22% of that for **3Be** (259 kJ mol<sup>-1</sup>). The value of  $\Delta E_{\text{DP}}$  for all other **3Ae** complexes is between 9–15% of that of **3Be**. Although the endothermic  $\Delta E_{\text{DP}}$  value for all **3Ae** species might suggest that these complexes would be stable in the condensed phase, this assumption does not account for the vaporization energies of the metals ( $\Delta E_{\text{V}}$ ) or **3Ae**/AeCp<sub>2</sub>. Indeed, when  $\Delta E_{\text{V}}$  is considered, only **3Be** is predicted to be amenable to isolation.<sup>18</sup> Considering limited kinetic stabilization afforded to the Ae–Ae bond by the Cp ligands, it seems probable that the other **3Ae** complexes would spontaneously disproportionate in the solid state. The homolytic Ae–Ae bond dissociation energies (BDEs) for the **3Ae** complexes decrease down the Ae group and are by far the highest for **3Be** (300 kJ mol<sup>-1</sup>). The BDE for **3Mg** (202 kJ mol<sup>-1</sup>) is only around 2/3 that of **3Be**.

Initial theoretical studies of Ae–Ae bonds assumed that these interactions would resemble conventional (weak) covalent, homopolar bonds.<sup>11</sup> Quantum theory of atoms-in-molecules (QTAIM) would describe such a conventional bond as possessing a (3, –1) bond critical point (BCP; a maximum of electron density in two dimensions and a minimum in the

third dimension) between the two Ae centres.<sup>12,23</sup> However, more recent computational studies indicate that this is not the case. Instead, Ae–Ae bonds are calculated to feature a (3, –3) critical point, or non-nuclear attractor (NNA), which corresponds to a large region of negative Laplacian.<sup>19,21</sup> In other words, a NNA is a local maximum in electron density that is not associated with the position of a specific nucleus. Hence, rather than being directly bonded to one another, each electro-positive Ae atom is “bonded” to the area of electron density associated with the NNA (Fig. 2). Indeed, QTAIM finds (3, –1) BCPs between each Ae atom and the NNA.<sup>19,21</sup> Experimental evidence for this phenomenon comes from high-resolution X-ray diffraction experiments performed on magnesium(i) dimers.<sup>12</sup> The implications of this bonding motif are wide-ranging. For example, the presence of the NNA is used to explain the highly reducing nature of complexes with Ae–Ae bonds.<sup>13</sup> Additionally, Mg–Mg bonds have been shown to be deformable, with a shallow bond potential energy surface, and have been crystallographically characterized over a wide range of distances (2.8 to >3.2 Å).<sup>24–27</sup>

From a molecular orbital standpoint, Be–Be and Mg–Mg bonds are calculated to be composed principally of contributions from the valence (*n*)s-orbitals, with a small degree of valence (*n*)p-orbital character, which varies depending on the supporting ligand set.<sup>13</sup> This is due to the relatively large energetic gap between the (*n*)s- and (*n*)p-orbitals. By contrast, a degree of d-orbital participation might be anticipated for the Ae–Ae bonds of heavier members of the group.<sup>28–30</sup> This is due to the fact that the (*n* – 1)d-orbitals are lower in energy than the (*n*)p-orbitals and the energy required to promote an electron from the (*n*)s-orbital to the (*n* – 1)d-orbitals is relatively small.

## Recent Advances

### Beryllium

Beryllium is the periodic table's second lightest metal, yet its chemistry is very poorly developed due to its extreme toxicity.<sup>31–33</sup> The Be<sup>2+</sup> ion is highly polarizing due to its enormous charge density (charge/radius ratio for Be<sup>2+</sup>: 6.45 Å<sup>-1</sup>; cf., Mg<sup>2+</sup>: 3.08 Å<sup>-1</sup>). Additionally, the element possesses extremely spatially concentrated frontier orbitals, which generally overlap effectively with the orbitals of other atoms in bonding interactions. As a result of these two factors, beryllium forms bonds with a significant degree of covalent character, which contrasts with the other Ae elements.<sup>20</sup> Consequently, of all the Ae elements, the potential for homometallic bonding would

**Table 1** Calculated ( $\omega$ B97X-D def2-TZVP) geometrical parameters, disproportionation energies ( $\Delta E_{\text{DP}}$ )<sup>a</sup> and homolytic Ae–Ae bond dissociation energies (BDEs)<sup>b</sup> for dimetalloenes (**3Ae**; Ae = Be, Mg, Ca, Sr, Ba), and metal vaporisation energies ( $\Delta E_{\text{V}}$ )<sup>19,22</sup>

M	<i>d</i> (Ae–Ae)/Å	$\Delta E_{\text{DP}}$ /kJ mol <sup>-1</sup>	$\Delta E_{\text{V}}$ /kJ mol <sup>-1</sup>	BDE/kJ mol <sup>-1</sup>
Be	2.06	259	309	300
Mg	2.81	58.2	132	202
Ca	3.75	38.2	153	123
Sr	4.11	22.3	141	106
Ba	4.52	33.6	149	90.9

<sup>a</sup>  $\Delta E_{\text{DP}}$  is for the gas phase reaction, CpAeAeCp → AeCp<sub>2</sub> + Ae. <sup>b</sup> BDE is calculated *via* the gas phase reaction, CpAeAeCp → 2 AeCp, where AeCp is a neutral radical.

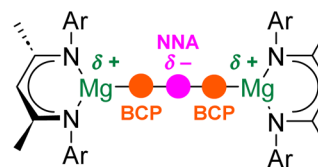


**Fig. 2** An illustration of the role of the non-nuclear attractor (NNA) in Ae–Ae bonding.



seem the greatest for beryllium. This is, indeed, consistent with the data presented in Table 1 and discussed above.<sup>19</sup> As a result, numerous synthetic and computational investigations into Be–Be bonding have been conducted over the past century.

Around 1930, Herzberg made the first attempts to prepare diberyllium ( $\text{Be}_2$ ) in the gas phase, which were unsuccessful.<sup>34</sup> The first spectroscopic identification of  $\text{Be}_2$  was carried out as late as 2009.<sup>35,36</sup> The synthesis of complex **3Be**, diberyllocene, was first examined in the 1970s; a benzene solution of  $\text{CpBeH}$  was heated in the presence of a platinum sheet in the hope of generating  $\text{H}_2$  and **3Be**.<sup>37</sup> However, no reaction was observed. Notably, several subsequent theoretical studies suggested that it might be possible to isolate **3Be** in the condensed phases.<sup>8,18</sup> More recently, inspired by the report of the first magnesium(i) dimers, the reduction of a range of beryllium(ii) complexes furnished with  $\beta$ -diketiminate or diamide ligands was attempted.<sup>24,38,39</sup> However, only products resulting from the activation of the ligand or the solvent were isolated.

In 2023 the first complex with a Be–Be bond was reported.<sup>40</sup> Reduction of beryllocene ( $\text{BeCp}_2$ ) with  $[(^{\text{Mes}}\text{Nacnac})\text{Mg}]_2$  ( $^{\text{Dipp}}\text{Nacnac} = \{[(\text{Mes})\text{NC}(\text{Me})_2\text{CH}]^-\}$ , Mes = 2,4,6-trimethylphenyl) produced  $(^{\text{Mes}}\text{Nacnac})\text{MgCp}$  and **3Be** in quantitative yield (Scheme 1). It is likely that  $(^{\text{Mes}}\text{Nacnac})\text{Mg}-\text{BeCp}$ , with a Mg–Be bond, is an intermediate in the formation of **3Be**.<sup>23</sup> Similarly to decamethylzincocene, **3Be** exhibits  $D_{5h}$  symmetry.<sup>7</sup> The crystallographically determined Be–Be bond distance in **3Be** (2.0545(18) Å) is within the range predicted by previous theoretical studies (2.041 to 2.077 Å).<sup>8,18,19,21</sup> Quantum chemical calculations indicate that the highest occupied molecular orbital (HOMO) of **3Be** corresponds to the Be–Be  $\sigma$ -bonding orbital.<sup>40</sup> The lowest unoccupied molecular orbital (LUMO) is principally ligand based, but the LUMO + 1 represents the Be–Be  $\sigma^*$ -antibonding combination. QTAIM calculations indicate that **3Be** also features a NNA in the Be–Be internuclear region.<sup>19</sup> Evidence for the expected reducing character of **3Be** was obtained through its reactions with aluminium- and zinc-iodides, which yield complexes with Be–Al and Be–Zn bonds, respectively, and  $\text{CpBeI}$ .<sup>40</sup>

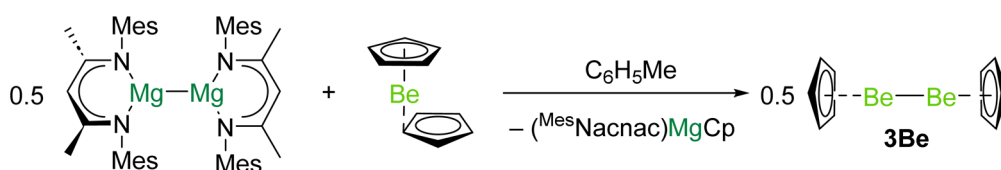
After the H–H  $\sigma$ -bond of  $\text{H}_2$ , the Be–Be bond is the simplest reported homoelemental bond with which synthetic chemistry could be performed. Comparisons with beryllium's neighbour in the Periodic Table, boron (and B–B bonds), can also be drawn. In this context, experimental studies of the Be–Be bond are of fundamental importance. For example, the oxidative addition chemistries of H–H and B–B bonds have been extremely intensively studied due to their relevance to catalytic

hydrogenation and borylation, respectively.<sup>41</sup> Is the oxidative addition of the Be–Be bond possible? Can  $\sigma$ -complexes of the Be–Be bond be prepared? Moreover, considering the relationship between beryllium and boron, is it possible to isolate complexes featuring Be–Be multiple bonds?<sup>42</sup> The one- and two-electron reduction of diborane(4) compounds, which are isoelectronic to beryllium(i) dimers, has been reported to yield species with B–B bond orders  $>1$ . Clearly, this is not likely to be a successful strategy in the case of **3Be**, as the lowest energy unoccupied orbital associated with the Be–Be bond is anti-bonding in character.<sup>40</sup> However, beryllium(i) dimers with alternative supporting ligands may possess Be–Be  $\pi$ -symmetry bonding orbitals that are of appropriate energy for population. Alternatively, theoretical studies have proposed that carbene-stabilized beryllium(0) dimers may be stable and would feature a Be=Be double bond with  $\sigma$ - and  $\pi$ -components.<sup>20,42</sup>

### Magnesium

Magnesium is vital to life on earth. It is the seventh most abundant element in the Earth's crust and is present in all cells of all organisms.<sup>43</sup> The magnesium(0) dimer,  $\text{Mg}_2$ , was first spectroscopically observed in 1970, sparking countless investigations into the properties of Ae diatomics.<sup>44</sup> Significantly, species with Mg–Mg bonds are implicated as intermediates in the formation of Grignard reagents, the mechanism for which remains uncertain.<sup>45,46</sup>

The study of complexes with Mg–Mg bonds has advanced rapidly over the past 15 years. Recent studies have focused on the design of complexes furnished with very bulky ligands to access new reactivity modes and structural motifs. For example, in 2021 it was reported that reduction of  $(^{\text{Dipep}}\text{Nacnac}^*)\text{MgI}$  ( $^{\text{Dipep}}\text{Nacnac}^* = \{[(\text{Dipep})\text{NC}(\text{tBu})_2\text{CH}]^-\}$ , Dipep = 2,6-diisopentylphenyl) with Na/NaCl gave the tetrametallic di-magnesium(0) complex  $\{[(^{\text{Dipep}}\text{Nacnac}^*)\text{Mg}]\text{Na}\}_2$  (**4**).<sup>47</sup> When **4** is dissolved in benzene and heated, sodium is extruded to yield  $\{[(^{\text{Dipep}}\text{Nacnac}^*)\text{Mg}]_2\text{Mg}\}$  (**5**), which features a linear tri-magnesium  $\text{Mg}^{\text{I}}-\text{Mg}^{\text{0}}-\text{Mg}^{\text{I}}$  core, formally consisting of a central magnesium(0) atom bonded to two magnesium(i) centres (Scheme 2). QTAIM calculations performed on **5** indicate that both Mg–Mg interactions feature a NNA, and yield charges of +1.00 for the central magnesium(0) atom and +1.22 for the flanking magnesium(i) centres. Additionally, quantum chemical calculations indicate that the extreme steric bulk of the  $[(^{\text{Dipep}}\text{Nacnac}^*)]^-$  ligand is key to the stability of **5**; the extrusion of magnesium(0) from this complex to yield  $[(^{\text{Dipep}}\text{Nacnac}^*)\text{Mg}]_2$  is calculated to be rather endothermic (141 kJ mol<sup>-1</sup>). With the smaller  $[(^{\text{Dipp}}\text{Nacnac})]^-$  ligand the ener-



**Scheme 1** Synthesis of diberyllocene (**3Be**), through reduction of beryllocene with a magnesium(i) dimer.





**Scheme 2** Formation of tri-magnesium complex **5**, which features a  $\text{Mg}^{\text{I}}\text{-Mg}^{\text{0}}\text{-Mg}^{\text{I}}$  core.

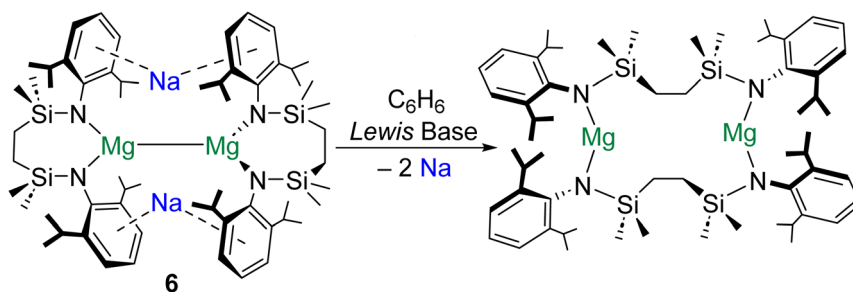
getic barrier to this process is much lower ( $10.5 \text{ kJ mol}^{-1}$ ). It is postulated by the authors that complex **5** may resemble an intermediate in Grignard reagent formation.

The extrusion of  $\text{Na}^{\text{0}}$  in the formation of **5** is testament to the reducing power of molecular magnesium(0) species.<sup>47</sup> Remarkably, similar behaviour has recently been described for magnesium(i) dimers. It was reported that addition of redox inert Lewis bases (e.g., THF) to magnesium(i) complex  $[\{\text{SiNDipp}\}\text{MgNa}]_2$  (**6**;  $[\text{SiNDipp}] = \{[\text{CH}_2\text{SiMe}_2\text{N}(\text{Dipp})]_2\}^{2-}$ ) induces the reduction of both  $\text{Na}^+$  ions to  $\text{Na}^{\text{0}}$ , with the concomitant oxidation of both  $\text{Mg}^{\text{I}}$  centres (Scheme 3).<sup>48</sup> It is proposed that the  $[\text{Na}_2\text{Mg}_2]^{2+}$  tetrametallic core of **6** is perturbed by coordination of THF to one of the  $\text{Na}^+$  centres in this complex. This precipitates the subsequent reduction of the unsolvated  $\text{Na}^+$  cation to  $\text{Na}^{\text{0}}$  by the electron density in the Mg–Mg bond. The energetic barrier to THF coordination at  $\text{Na}^+$  ( $21.3 \text{ kJ mol}^{-1}$ ) is far lower than that associated with coordination of the donor solvent to  $\text{Mg}^+$  ( $108 \text{ kJ mol}^{-1}$ ). Notably, the Mg–Mg bond in complex **6** is very long ( $>3.2 \text{ \AA}$ ).<sup>26</sup> Perhaps as a consequence, QTAIM calculations performed on **6** do not locate a NNA for the Mg–Mg interaction, but find instead a single BCP between the magnesium centres and BCPs between this point and the  $\text{Na}^+$  cations. Remarkably, although the electron density at the (Mg–Mg)–Na BCP is very low ( $\rho = 0.003$ ), these interactions are calculated to play an important stabilizing role in **6** ( $105 \text{ kJ mol}^{-1}$  each). Notably, the largely electrostatic nature of the (Mg–Mg)–Na interaction in **6** differs from the more covalent Mg–Na bonding in **4** ( $\rho = 0.010\text{--}0.015$ ).<sup>47</sup> QTAIM calculations return very low charges for both magnesium centres in **6** ( $+0.97$ ), which are comparable to that of the formal magnesium(0) centre in **5** ( $+1.00$ ).<sup>47</sup>

Complex **6** is reported to activate  $\text{H}_2$  and reduce CO to ethynediolate.<sup>49</sup>

The preparation of **4** (and its reactivity to form **5**), as well as the reactivity of **6**, highlight the importance of counterion and reductant.<sup>50</sup> In the case of **4** and **6**,  $\text{Na}^+$  cations play key structural roles (through Na–aryl interactions), which contribute to the kinetic stabilization of the reactive sites in these complexes. Additionally, Mg–Na interactions lessen the accumulation of negative charge at the Mg centres in **4** and the Mg–Mg bond of **6**, also stabilizing both complexes. It seems likely that future progress in this area will rely upon the synergy of low-valent Ae centres/Ae–Ae bonds and alkali metal counterions to engender novel reactivity.

Ongoing investigations into  $\beta$ -diketiminate-ligated magnesium(i) dimers continue to yield remarkable results. For example, coordination of a Lewis base to one of the magnesium(i) centres within **1** lengthens the Mg–Mg linkage and increases its reactivity. These singly “donor-activated” complexes possess a three-coordinate magnesium(i) centre that can coordinate a substrate. Resultantly, they are more reactive than symmetrically doubly donor-coordinated complexes in which both magnesium(i) centres are coordinatively saturated. In evidence of this,  $[(^{\text{Dipp}}\text{Nacnac})(\text{D})\text{Mg}\text{-Mg}(\text{D}^{\text{Dipp}}\text{Nacnac})]$  (D = 4-dimethylaminopyridine or 1,3,4,5-tetramethyl-imidazol-2-ylidene) is capable of facilitating the reductive cyclotrimerization of CO, forming the deltate dianion,  $[\text{C}_3\text{O}_3]^{2-}$ .<sup>51</sup> In other work, it has also been demonstrated that photolysis of **1** leads to Mg–Mg bond cleavage and generation of highly reactive magnesium(i) radicals, which have evaded isolation.<sup>52</sup> However, these radicals are capable of the “Birch-like” two-electron reduction and C–H bond activation of benzene, the



**Scheme 3** Extrusion of metallic sodium through addition of Lewis bases to magnesium(i) dimer complex **6**.





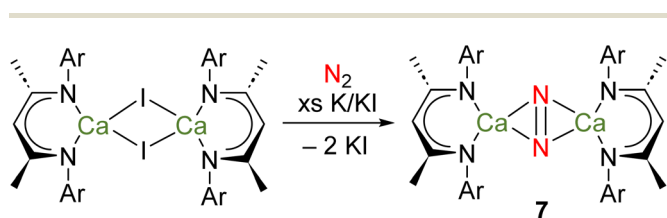
regio- and chemo-selective C–H bond activation of toluene and xylene, and the defluorination of fluorobenzene. Although several other fleeting, highly reactive magnesium(i) radical complexes have been reported, none are believed to possess Mg–Mg bonds, or be generated from species with Mg–Mg bonds.<sup>27,53–55</sup>

Future work will likely continue to leverage the deformability of the Mg–Mg interaction in order to engender new reactivity. For example, there is scope for the deployment of bridging ligands that enforce a specific Mg–Mg separation in order to modulate reactivity of the linkage.

### Calcium and the heavier alkaline earth elements (Sr–Ra)

Calcium is the fifth most abundant element in the Earth's crust and the most abundant metal in the human body, with a range of crucial biochemical roles. Strontium and barium are also both abundant elements – the 15<sup>th</sup> and 14<sup>th</sup> most abundant in the Earth's crust, respectively. Due to its similarities with Ca, Sr is rather biologically benign.<sup>43</sup> However, it is believed Ba<sup>2+</sup> blocks K<sup>+</sup> channels in the body, meaning that water-soluble Ba compounds are toxic.<sup>43</sup> Due to their large ionic radii and polarized bonding, many coordination complexes of heavier Ae elements are labile and prone to Schlenk-type equilibria.

Several attempts to prepare stable complexes featuring homometallic bonds of the heavier Ae elements have been described, although none have been successful.<sup>24</sup> Perhaps most notably, it was recently reported that reduction of  $[(^{\text{Dipep}}\text{Nacnac})\text{CaI}]_2$ , in methylcyclohexane and under an atmosphere of dinitrogen, yields the complex  $\{[(^{\text{Dipep}}\text{Nacnac})\text{Ca}]_2(\mu\text{-N}_2)\}$  (**7**), which could be crystallographically characterized as



**Scheme 4** Attempted preparation of a complex with a Ca–Ca bond, instead leading to formation of di-calcium dinitrogen complex **7**.

its bis(tetrahydrofuran) and bis(tetrahydropyran) adducts (Scheme 4).<sup>56</sup> Although a complex with a Ca–Ca bond was the target of these investigations, there is no evidence to suggest such a species is an intermediate in the formation of **7**. Indeed, given the low BDE of a hypothetical Ca–Ca bond (*e.g.*, 123 kJ mol<sup>−1</sup> for **3Ca**), other possibilities should be considered.<sup>19</sup> For example, the similarities between rare-earth elements and heavier Ae elements are manifold – the elements are powerful reductants and their bonding interactions are highly polarized. Indeed, divalent rare-earth complexes that do not feature M–M bonds are known to activate N<sub>2</sub>.<sup>57</sup> Furthermore, computational evidence suggests that partially occupied calcium-based d-orbitals may be responsible for the binding of N<sub>2</sub>, as is believed to be key for rare-earth complexes.<sup>56,57</sup> Thus, it is possible that the reduction of N<sub>2</sub> is carried out by a mononuclear calcium(i) radical, or a molecular calcium(0) species analogous to complex **4**.

Actinide-actinide and lanthanide-lanthanide bonds are predicted to be very weak, similarly to homometallic bonds between heavy alkaline earth elements (Table 1). However, the first complexes with actinide-actinide and lanthanide-lanthanide bonds, which are supported by bridging ligands, have been reported recently.<sup>58,59</sup> Therefore, analogous strategies for the synthesis of heavier Ae–Ae bonds might be attempted. It has been demonstrated that a set of six bridging halide ligands – a pair between each pair of metal centres – will hold three thorium ions within a proximity which enables three-centre two-electron tri-thorium bonding (**8**, Fig. 3).<sup>58</sup> This approach was subsequently applied for the preparation of a range of complexes with halide-supported lanthanide-lanthanide bonds (**9**, Fig. 3).<sup>59</sup> Significantly, (supported) two-centre one-electron (**10**, Fig. 3) and three-centre one-electron homometallic bonding of the rare-earth element yttrium, which is adjacent to strontium in the Periodic Table, has been described.<sup>60</sup> The homometallic rare-earth element bonds are all calculated to principally comprise contributions from metal d-orbitals, as might be predicted for Ca, Sr, and Ba.<sup>28</sup> In the case of Ra, however, relativistic effects destabilize the 6d-orbital manifold.<sup>61</sup> As a result, Ra–Ra bonding might be expected to principally comprise contributions from the 7s- and 7p-orbitals.<sup>4</sup> This contrasts with the Th–Th bonding of **8**, which is calculated to be primarily of Th 6d-orbital character

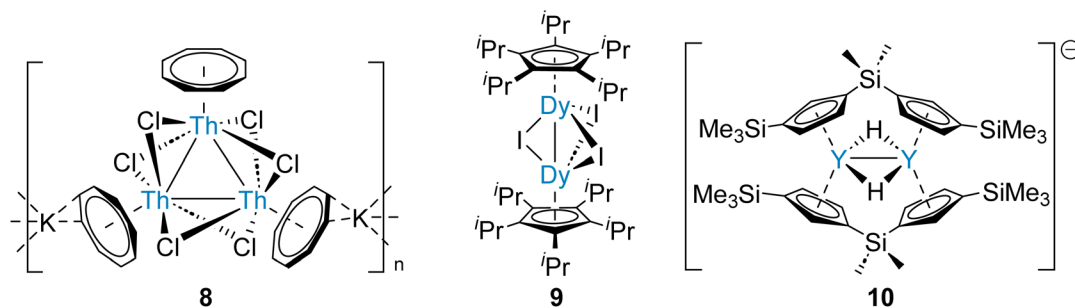


**Fig. 3** Rare-earth and actinide complexes that feature supported M–M bonds – a strategy which may be employed for the preparation of stable complexes that feature heavier Ae–Ae bonds.



(80%).<sup>58</sup> Considering the proximity of Ra (element 88) and Th (element 90) within the Periodic Table, this dissimilarity is striking.

Successful preparation of heavier Ae–Ae bonds may also depend on judicious selection of starting materials and synthetic methodology. For example, reduction of higher-valent elements with alkali metals can lead to the formation of ill-defined product mixtures. Thus, the +1-oxidation state of the heavier Ae elements might be accessed more straightforwardly by the one-electron oxidation of the metal (in the presence of a suitable supporting ligand), rather than reduction of a divalent Ae precursor.<sup>62,63</sup>

## Future directions

The synthesis of **5** demonstrates that clusters comprising several Ae–Ae bonds might be isolable.<sup>64</sup> In this context, electrospray mass spectrometry has previously been used to detect an ion with a likely composition of  $[\text{Mg}_{16}\text{Cp}^*_8\text{Br}_4\text{K}]^-$  from the reaction of metastable “MgBr” with  $\text{KCp}^*$ .<sup>65</sup> Although no crystallographic data for this species could be obtained, a possible structure was derived from quantum chemical calculations, featuring a  $\text{Mg}_{14}$  core, consisting of 27 Mg–Mg bonds, resembling hexagonal close-packed Mg metal. The structural characterization of these clusters would serve to further elucidate the possible pathways for Grignard reagent formation.<sup>66</sup> In this context, with the report of **3Be** and the relatively high strength of Be–Be bonds, it may be possible to prepare catenated chains of beryllium atoms. This has previously been suggested to be feasible by theoretical investigations of multi-beryllocenes (*i.e.*,  $\text{CpBe}_n\text{Cp}$ ;  $n = 3,4,5$ ).<sup>18</sup> Alternatively, rings of Be atoms connected by Be–Be bonds may be synthesised. This also presents the possibility of all-Ae metal aromaticity.

As previously mentioned, species that feature Ae–Ae multiple bonding interactions are feasible synthetic targets, particularly in the case of Be and Mg.<sup>20</sup> Indeed, the LUMO and LUMO + 1 of many magnesium(i) dimers correspond to  $\pi$ -symmetry Mg–Mg bonding orbitals.<sup>9</sup> Thus, shrewd ligand design may allow for the one- or two-electron population of these orbitals.

## Conclusions and outlook

Considering the apparent modularity and high reactivity of complexes that feature Mg–Mg bonds, it seems likely that research into these species will continue to flourish. Indeed, such complexes have already been shown to be capable of reactivity that is currently unknown for transition metals, such as the cyclotrimerization of CO.<sup>51</sup> Although the synthetic study of Be–Be bonding is in its infancy, this will likely yield many striking discoveries.<sup>40</sup> Certainly, a comprehensive understanding of beryllium’s chemistry is necessary in order to test models of bonding, which are primarily based on the properties of the simplest elements.

The isolation of complexes with homometallic actinide and rare-earth bonding suggests new approaches for the preparation of Ae–Ae bonds for the heavier elements of the group.<sup>58–60</sup> It seems possible that, to access many of these highly reactive species, ligands that impart sufficient solubility to facilitate their preparation in inert alkane solvents, or the use of mechanochemical synthetic methods, will be necessary.

## Conflicts of interest

There are no conflicts to declare.

## Acknowledgements

J. T. B. thanks St John’s College, Oxford, for a Junior Research Fellowship, as well as the John Fell Fund (0011792) and the Royal Society of Chemistry (Research Fund R23-3176939355) for financial support. Mr L. P. Griffin, Dr L. R. Thomas-Hargreaves, and Prof. S. Aldridge are thanked for constructive and insightful discussions.

## References

- 1 E. Vangioni-flam and M. Cassé, *Astrophys. Space Sci.*, 1999, **11**, 77–86.
- 2 S. Freeman, *Encyclopedia of Inorganic and Bioinorganic Chemistry*, Wiley, 2015, pp. 1–11.
- 3 P. Curie, M. Curie and G. Bémont, *C. R. Acad. Sci.*, 1898, **127**, 1215–1217.
- 4 F. D. White, N. A. Thiele, M. E. Simms and S. K. Cary, *Nat. Chem.*, 2023, DOI: [10.1038/s41557-023-01366-z](https://doi.org/10.1038/s41557-023-01366-z).
- 5 M. S. Hill, D. J. Liptrot and C. Weetman, *Chem. Soc. Rev.*, 2016, **45**, 972–988.
- 6 S. Harder, *Chem. Rev.*, 2010, **110**, 3852–3876.
- 7 I. Resa, E. Carmona, E. Gutierrez-Puebla and A. Monge, *Science*, 2004, **305**, 1136–1138.
- 8 Y. Xie, H. F. Schaefer and E. D. Jemmis, *Chem. Phys. Lett.*, 2005, **402**, 414–421.
- 9 S. P. Green, C. Jones and A. Stasch, *Science*, 2007, **318**, 1754–1757.
- 10 A. Stasch and C. Jones, *Dalton Trans.*, 2011, **40**, 5659.
- 11 J. Overgaard, C. Jones, A. Stasch and B. B. Iversen, *J. Am. Chem. Soc.*, 2009, **131**, 4208–4209.
- 12 J. A. Platts, J. Overgaard, C. Jones, B. B. Iversen and A. Stasch, *J. Phys. Chem. A*, 2011, **115**, 194–200.
- 13 C. Jones, *Nat. Rev. Chem.*, 2017, **1**, 0059.
- 14 B. Rösch and S. Harder, *Chem. Commun.*, 2021, **57**, 9354–9365.
- 15 C. Jones, *Commun. Chem.*, 2020, **3**, 8–11.
- 16 L. A. Freeman, J. E. Walley and R. J. Gilliard, *Nat. Synth.*, 2022, **1**, 439–448.
- 17 S. Li, X.-J. Yang, Y. Liu, Y. Zhao, Q.-S. Li, Y. Xie, H. F. Schaefer and B. Wu, *Organometallics*, 2011, **30**, 3113–3118.



- 18 A. Velazquez, I. Fernández, G. Frenking and G. Merino, *Organometallics*, 2007, **26**, 4731–4736.
- 19 M. A. Gosch and D. J. D. Wilson, *Organometallics*, 2023, **42**, 2185–2196.
- 20 S. A. Couchman, N. Holzmann, G. Frenking, D. J. D. Wilson and J. L. Dutton, *Dalton Trans.*, 2013, **42**, 11375–11384.
- 21 X. Li, S. Huo, Y. Zeng, Z. Sun, S. Zheng and L. Meng, *Organometallics*, 2013, **32**, 1060–1066.
- 22 Y. Zhang, J. R. G. Evans and S. Yang, *J. Chem. Eng. Data*, 2011, **56**, 328–337.
- 23 J. T. Boronski, L. R. Thomas-Hargreaves, M. A. Ellwanger, A. E. Crumpton, J. Hicks, D. F. Bekiş, S. Aldridge and M. R. Buchner, *J. Am. Chem. Soc.*, 2023, **145**, 4408–4413.
- 24 S. J. Bonyhady, C. Jones, S. Nembenna, A. Stasch, A. J. Edwards and G. J. McIntyre, *Chem. – Eur. J.*, 2010, **16**, 938–955.
- 25 S. P. Green, C. Jones and A. Stasch, *Angew. Chem., Int. Ed.*, 2008, **47**, 9079–9083.
- 26 H.-Y. Liu, R. J. Schwamm, S. E. Neale, M. S. Hill, C. L. McMullin and M. F. Mahon, *J. Am. Chem. Soc.*, 2021, **143**, 17851–17856.
- 27 T. X. Gentner, B. Rösch, G. Ballmann, J. Langer, H. Elsen and S. Harder, *Angew. Chem., Int. Ed.*, 2019, **58**, 607–611.
- 28 M. Zhou and G. Frenking, *Acc. Chem. Res.*, 2021, **54**, 3071–3082.
- 29 X. Wu, L. Zhao, D. Jiang, I. Fernández, R. Berger, M. Zhou and G. Frenking, *Angew. Chem., Int. Ed.*, 2018, **57**, 3974–3980.
- 30 I. Fernández, N. Holzmann and G. Frenking, *Chem. – Eur. J.*, 2020, **26**, 14194–14210.
- 31 M. R. Buchner, *Chem. Commun.*, 2020, **56**, 8895–8907.
- 32 M. R. Buchner, *Chem. – Eur. J.*, 2019, **25**, 12018–12036.
- 33 D. Naglav, M. R. Buchner, G. Bendt, F. Kraus and S. Schulz, *Angew. Chem., Int. Ed.*, 2016, **55**, 10562–10576.
- 34 G. Herzberg, *Z. Med. Phys.*, 1929, **57**, 601–630.
- 35 J. M. Merritt, V. E. Bondybey and M. C. Heaven, *Science*, 2009, **324**, 1548–1551.
- 36 K. Patkowski, V. Špirko and K. Szalewicz, *Science*, 2009, **326**, 1382–1384.
- 37 H. Schmidbaur, *Be Organoberyllium Compounds*, Springer Berlin Heidelberg, Berlin, Heidelberg, 1987, vol. 21.
- 38 M. Arrowsmith, M. S. Hill, G. Kociok-Köhn, D. J. MacDougall, M. F. Mahon and I. Mallov, *Inorg. Chem.*, 2012, **51**, 13408–13418.
- 39 K. G. Pearce, M. S. Hill and M. F. Mahon, *Chem. Commun.*, 2023, **59**, 1453–1456.
- 40 J. T. Boronski, A. E. Crumpton, L. L. Wales and S. Aldridge, *Science*, 2023, **380**, 1147–1149.
- 41 J. A. Labinger, *Organometallics*, 2015, **34**, 4784–4795.
- 42 H. Braunschweig and R. D. Dewhurst, *Organometallics*, 2014, **33**, 6271–6277.
- 43 R. Crichton, *Biological Inorganic Chemistry*, Elsevier, 2019.
- 44 W. J. Balfour and A. E. Douglas, *Can. J. Phys.*, 1970, **48**, 901–914.
- 45 Y. Imizu and K. J. Klabunde, *Inorg. Chem.*, 1984, **23**, 3602–3605.
- 46 L. A. Tjurina, V. V. Smirnov, D. A. Potapov, S. A. Nikolaev, S. E. Esipov and I. P. Beletskaya, *Organometallics*, 2004, **23**, 1349–1351.
- 47 B. Rösch, T. X. Gentner, J. Eysel, J. Langer, H. Elsen and S. Harder, *Nature*, 2021, **592**, 717–721.
- 48 H. Y. Liu, S. E. Neale, M. S. Hill, M. F. Mahon, C. L. McMullin and E. Richards, *Angew. Chem., Int. Ed.*, 2022, e202213670, DOI: [10.1002/anie.202213670](https://doi.org/10.1002/anie.202213670).
- 49 H. Y. Liu, S. E. Neale, M. S. Hill, M. F. Mahon, C. L. McMullin and B. L. Morrison, *Chem. Commun.*, 2023, **59**, 3846–3849.
- 50 J. Hicks, M. Juckel, A. Paparo, D. Dange and C. Jones, *Organometallics*, 2018, **37**, 4810–4813.
- 51 K. Yuvaraj, I. Douair, A. Paparo, L. Maron and C. Jones, *J. Am. Chem. Soc.*, 2019, **141**, 8764–8768.
- 52 D. D. L. Jones, I. Douair, L. Maron and C. Jones, *Angew. Chem., Int. Ed.*, 2021, **60**, 7087–7092.
- 53 D. Jędrzkiewicz, J. Mai, J. Langer, Z. Mathe, N. Patel, S. DeBeer and S. Harder, *Angew. Chem., Int. Ed.*, 2022, e202200511, DOI: [10.1002/anie.202200511](https://doi.org/10.1002/anie.202200511).
- 54 R. Mondal, M. J. Evans, T. Rajeshkumar, L. Maron and C. Jones, *Angew. Chem., Int. Ed.*, 2023, e202308347, DOI: [10.1002/anie.202308347](https://doi.org/10.1002/anie.202308347).
- 55 D. Jędrzkiewicz, J. Langer and S. Harder, *Z. Anorg. Allg. Chem.*, 2022, **648**, 16–19.
- 56 B. Rösch, T. X. Gentner, J. Langer, C. Färber, J. Eysel, L. Zhao, C. Ding, G. Frenking and S. Harder, *Science*, 2021, **371**, 1125–1128.
- 57 A. J. Ryan, S. Ganesh Balasubramani, J. W. Ziller, F. Furche and W. J. Evans, *J. Am. Chem. Soc.*, 2020, **142**, 9302–9313.
- 58 J. T. Boronski, J. A. Seed, D. Hunger, A. W. Woodward, J. van Slageren, A. J. Woolees, L. S. Natrajan, N. Kaltsoyannis and S. T. Liddle, *Nature*, 2021, **598**, 72–75.
- 59 Z. Zhu and J. Tang, *Chem. Soc. Rev.*, 2022, **51**, 9469–9481.
- 60 J. C. Wedal, L. M. Anderson-Sanchez, M. T. Dumas, C. A. Gould, M. J. Beltrán-Leiva, C. Celis-Barros, D. Páez-Hernández, J. W. Ziller, J. R. Long and W. J. Evans, *J. Am. Chem. Soc.*, 2023, **145**, 10730–10742.
- 61 U. Dammalapati, K. Jungmann and L. Willmann, *J. Phys. Chem. Ref. Data*, 2016, **45**, 013101.
- 62 M. Schorpp and I. Krossing, *Chem. Sci.*, 2020, **11**, 2068–2076.
- 63 G. Wang, J. E. Walley, D. A. Dickie, S. Pan, G. Frenking and R. J. Gilliard, *J. Am. Chem. Soc.*, 2020, **142**, 4560–4564.
- 64 R. Köppe, P. Henke and H. Schnöckel, *Angew. Chem., Int. Ed.*, 2008, **47**, 8740–8744.
- 65 T. Kruczyński, F. Henke, M. Neumaier, K. H. Bowen and H. Schnöckel, *Chem. Sci.*, 2016, **7**, 1543–1547.
- 66 T. Kruczyński, N. Pushkarevsky, P. Henke, R. Köppe, E. Baum, S. Konchenko, J. Pikies and H. Schnöckel, *Angew. Chem., Int. Ed.*, 2012, **51**, 9025–9029.

